


 Cite this: *RSC Adv.*, 2025, 15, 2947

# Alum sludge-driven electro-phytoremediation in constructed wetlands: a novel approach for sustainable nutrient removal†

 Daryoush Sanaei, <sup>a</sup> Amir Mirshafiee <sup>\*bc</sup> and Amir Adibzadeh<sup>bc</sup>

In addition to their advantages as promising methods for wastewater treatment, CWs exhibit poor performance in terms of N and P removal efficiency in the effluent of wastewater treatment plants. By focusing on this issue, we designed CWs integrated with a biochar-doped activated carbon cloth (ACC) electrode and alum sludge from water treatment plants as a substrate to achieve concomitant organic matter and nutrient removal efficiency. Compared with the use of one layer of alum sludge in CWs (CWs-C3) with ACC electrodes inserted in two layers, which uses one layer of alum sludge, a significant improvement in removal efficiency was achieved (96% for COD; 89% for TN; and 77% for TP). The findings revealed that the application of potential accompanied by the insertion of a cathode ACC electrode into the first layer of alum sludge was beneficial for completing nitrification and facilitating denitrification in the cathode and anode regions, respectively, resulting in increased removal of organic matter and nutrients. Further evaluation revealed that the TN-TP synergetic removal mechanism was influenced by the use of Fe<sup>2+</sup> as an electron donor and as a driving force for the development of autotrophic denitrifying bacteria to increase nitrate reduction. Additionally, the formation of FePO<sub>4</sub> and AlPO<sub>4</sub> and their adsorption through the interaction of FeOOH and AlOOH with phosphate constitute the main removal mechanism for TP in wastewater. Another reason for the increased removal efficiency in the CW-C3 reactor was the greater abundance and microbial diversity effectuated by the application of potential in the anode and cathode regions. In summary, a promising strategy for simultaneously promoting organic matter and nutrients and utilizing CWs on a large scale and in practical applications was proposed.

Received 11th November 2024

Accepted 13th January 2025

DOI: 10.1039/d4ra08021a

[rsc.li/rsc-advances](https://rsc.li/rsc-advances)

## 1. Introduction

The enormous and varied production of wastewater engendered by rapid economic and population growth, development urbanization and industrialization, in addition to the increasing utilization of fossil resources as both carbon and energy sources, has led to crucially rising issues across the globe. Harmful environmental discharge, water crises, energy scarcity, climate change, and global warming are consequences of the abovementioned issues.<sup>1</sup> The generated wastewaters can be treated chemically or biologically using various methods to limit their adverse effects on the environment and natural resources. Most applied technologies require further

sophisticated processes to remove or mitigate side products and sludge before being discharged into the environment.<sup>2</sup> Additionally, wastewater treatment facilities that involve carbon-based and nutrient removal not only lead to the production of greenhouse gases (GHGs) but also indirectly contribute to energy consumption by various equipment and sludge handling and treatment methods.<sup>3</sup>

Notably, nutrients such as nitrate and phosphorus, which are major components of wastewater, can cause excessive plant growth and eutrophication through entry into the environment and water bodies owing to incomplete treatment. This can further lead to the need for chemical or biological processes for mitigation at the standard level and increase capital and operational costs and energy consumption.<sup>4</sup> To limit clean water resources, the ability to enter plastics and other pollutants in the environment, GHG and energy consumption, and pervasive mismanaging of wastewater-treated wastes, the development of environmentally friendly technology and an aspiration of clean water and energy have led to an increasing emphasis on less carbonization and less energizing wastewater treatment and infrastructure.<sup>5</sup>

<sup>a</sup>Student Research Committee, Baqiyatallah University of Medical Sciences, Tehran, Iran. E-mail: daryoushsanaei@gmail.com

<sup>b</sup>Health Research Center, Life Style Institute, Baqiyatallah University of Medical Sciences, Tehran, Iran. E-mail: a\_mirsh1@yahoo.com

<sup>c</sup>Department of Environmental Health Engineering, Faculty of Health, Baqiyatallah University of Medical Sciences, Tehran, Iran

† Electronic supplementary information (ESI) available. See DOI: <https://doi.org/10.1039/d4ra08021a>



The nature-based solution coupled with advanced technologies such as constructed wetlands (CWs) is a state-of-the-art technology performed worldwide, particularly for treating different types of wastewaters at scales ranging from small and rural communities to urban and industrial applications.<sup>6</sup> As a green, eco-friendly, low-cost and easy maintenance method for treating wastewater, CWs are widely attracted and widely applied worldwide. This study aims to enhance the effectiveness of CWs by addressing the limitations of existing methods and introducing novel substrates and configurations to improve nutrient and organic matter removal. As this technology has all the hallmarks of ideal and effective wastewater treatment, Marwa *et al.*<sup>7</sup> compared the wastewater treatment performances of CWs with two types of configurations (vertical flow and horizontal flow). They concluded that in terms of the removal rates of BOD, COD, TSS, TN, TP and NH<sub>4</sub>, both configurations of CWs were attained with sparingly higher removal efficiencies of 77% and 68% in the case of vertical flow than in the case of horizontal flow. The study revealed that the type of substrate, retention time and plant species can be considered the most dominant variables controlling CW performance. Moreover, CWs can be performed for particular wastewater with organic or inorganic pollutants. For example, Fazila Younas *et al.*<sup>8</sup> evaluated the utilization of CWs to treat the tannery industry, which contains high concentrations of chromium (Cr). They reported that the dominant parameters for achieving a high removal rate of Cr *via* CWs are wetland plants and the type of substrate used as media. The Cr removal efficiency reached 80 to 99% when all types of configurations of CWs were used. However, the horizontal flow and vertical flow modes do not consider actual operating conditions, unlike the free water surface CW mode.

Conventional CWs, from a treatment perspective, have poor N and P removal performance in wastewater effluent and do not have enough time to degrade organic matter in wastewater as much as other methods can.<sup>9</sup> Thus, to meet the requirements of improved treatment efficiency, various strategies, such as the introduction of novel and effective substrates in single or multilayer systems and different plants, the establishment of a microbial community in a fixed bed, and the integration of other wastewater treatment technologies, are widely recommended and investigated.<sup>10</sup> A study was performed to successfully remediate phosphorus from wastewater *via* a novel composite substrate containing brick waste, tile waste and gravel in CWs.<sup>11</sup> The total phosphorus and phosphate removal efficiencies from domestic wastewater were reported to be 72% and 78%, respectively. Additionally, the coupling of CWs with other systems for improving the performance of bioremediation of organic matter and nutrients has been investigated, particularly in the last few decades.<sup>12</sup> Among many examples, Mengni Tao *et al.*<sup>13</sup> utilized high-density polyethylene (HDPE) fillers as effective substrates coupled with microbial fuel cells (MFCs) for simultaneous bioelectricity generation and enhanced nitrogen removal for the treatment of low-carbon wastewater. A 97.55% total nitrogen removal and bioelectricity generation with a power density of 2.22 mW m<sup>-2</sup> were achieved

with the addition of both HDPE fillers and *Acorus calamus* biomass in coupled CWs-MFCs.

Considering the nature and concentration of organic matter/nutrients, an evaluation of the performance of CWs with water alum sludge with a carbon cloth electrode doped with biochar for improving the performance of CWs for nutrient and organic matter removal from domestic wastewater was performed. The application of alum sludge as a cost-effective substrate in this study demonstrated a uniform dispersion of metal species. This substrate proved to be highly effective in removing organic matter, nitrogen (N), and phosphorus (P), attributed to the abundant hydroxide sites that facilitate interactions and accelerate redox reactions. Furthermore, the incorporation of a biochar-coated carbon cloth electrode, alongside current application, resulted in significant removal rates. This success is due to the creation of regions within the substrate that fostered microbial growth and provided an ideal medium for biofilm formation. The findings indicated that the enhanced growth and biofilm formation observed in this study led to lower rates of nitrification-denitrification under these conditions, compared to those without an electrode. Consequently, the stable Fe–Al–N (or P) cycle within the alum sludge substrate, combined with the formation of active zones near the electrodes, accelerated biofilm formation and achieved efficient removal of nitrogen and phosphorus.

## 2. Materials and methods

### 2.1. Chemicals

**2.1.1. Preparation and characterization of substrates.** The alum sludge was collected from a water clarification plant located at conventional water treatment plant no. 1 of Tehran, Iran. After air drying, the samples were gently ground. The resulting dried sludge alum was passed through a 2 mm sieve, and the characteristic properties of the obtained alum sludge are shown in Table 1.

**2.1.2. Preparation and characterization of the CC-modified biochar electrode.** Before biochar-doped CC electrodes are prepared, the biochar is obtained *via* carbonization and activation of coconut shell fibers. Initially, coconut was purchased from a fruit market, Tehran, Iran, and its fibers were separated from the shell and washed thoroughly with tap water or distilled water. The washed fibers were subsequently dried at 105 °C in an oven overnight. The dried fibers were powdered in Porcelain to reach the millimetric size of the particles. Carbonization was performed under an inert atmosphere (N<sub>2</sub> at 100 mL min<sup>-1</sup>) in a tube furnace at 750 °C with a heating rate of 10 °C min<sup>-1</sup> for 2 h. After the prepared biochar subsequently reached room temperature, activation was carried out by placing the prepared biochar in a vacuum oven at 100 °C.

Carbon cloth (CC) was used as an electrode and was purchased from Redox Kala, Iran. To remove impurities, the carbon cloth (2 × 2 cm) was soaked and sonicated in acetone, ethanol, or 0.2 M HCl for 30 min each. After sonication, the CC was rinsed with DW several times and then dried in air at room temperature. To increase the stability and strongly bind the



Table 1 The characteristic properties of water treatment-based alum sludges

Parameters	units	Mean $\pm$ SD	Measuring method
pH	—	6.9 $\pm$ 0.2	pH meter (model 111)
VSS/SS	%	0.27 $\pm$ 0.25	In all analytical procedures for determination of suspended solids (SS), weighed filters are used for sample filtration, the filters are dried at approximately 105 °C after filtration, cooled in a desiccator to room temperature and the weight of the loaded filter is determined A sample is filtered through a glass fiber filter with 1.5 micron openings. The filter is dried in an oven at 103 °C for 24 hours (TSS), and then placed in a 550 °C furnace for 1 hour (VSS) <sup>14</sup>
TOC	g kg <sup>-1</sup>	116 $\pm$ 19	Shimadzu TOC-VCSH total organic carbon analyzer
BET	g m <sup>-2</sup>	122 $\pm$ 39	The N <sub>2</sub> adsorption/desorption measurements with the use of an ASAP 2020 micromeritics instrument
Total P	g kg <sup>-1</sup>	1.4 $\pm$ 1.1	Analyzed following method 365.1 (ref. 15)
Ca	g kg <sup>-1</sup>	15.6 $\pm$ 6.2	One gram of each dried residual was digested with 30 mL of HCl, 10 mL HNO <sub>3</sub> , 5 mL HF, and 2 mL HClO <sub>4</sub> on a hotplate and analyzed with ICP-AES (Varian, Vista Pro) according to method 6010C <sup>16</sup>
Total Al	g kg <sup>-1</sup>	155 $\pm$ 18	One gram of each dried residual was digested with 30 mL of HCl, 10 mL HNO <sub>3</sub> , 5 mL HF, and 2 mL HClO <sub>4</sub> on a hotplate and analyzed with ICP-AES (Varian, Vista Pro) according to method 6010C <sup>16</sup>
Total Fe	g kg <sup>-1</sup>	6.2 $\pm$ 2.5	One gram of each dried residual was digested with 30 mL of HCl, 10 mL HNO <sub>3</sub> , 5 mL HF, and 2 mL HClO <sub>4</sub> on a hotplate and analyzed with ICP-AES (Varian, Vista Pro) according to method 6010C <sup>16</sup>
SO <sub>4</sub> <sup>2-</sup>	g kg <sup>-1</sup>	7.8 $\pm$ 0.28	Sulfate results were measured using spectrophotometry (DR - 4000, Hach Co., Coveland Co.)
Cl <sup>-</sup>	g kg <sup>-1</sup>	16.4 $\pm$ 0.55	Determined as described in ref. 17
Moisture content	%	34.59 $\pm$ 1.5	Alum sludge samples were dried in an oven at 103 $\pm$ 2 °C for 72 h to determine the moisture content

biochar on the carbon cloth electrode, CC was activated for 1 h at 100 °C in a vacuum oven to prepare activated carbon cloth (ACC) before use. To coat ACC with biochar, an ink material was prepared by dispersing 100 mg of biochar in a mixture of 50  $\mu$ L of 5% Nafion solution and 500  $\mu$ L of isopropyl alcohol: water mixture (3 : 1 V/V), and the mixture was sonicated in an ultrasonic bath for 30 min to form homogeneous ink. The resulting ink was drop-cast on an ACC electrode (2  $\times$  2 cm) *via* the air brushing method. The prepared electrode-coated biochar was dried in air overnight. The amount of biochar loaded on the ACC was 45 mg cm<sup>-2</sup>. Copper wire was used to connect the electrode of the cathode and anode, and a power supply was applied to provide the required current.

## 2.2. CWs setup and operation

The CWs were constructed from cylindrical Plexiglas with a diameter of 5 cm and height of 38 cm with an outlet pipe at the bottom (Fig. 1). A stainless-steel mesh was placed at the bottom of the column just 1.5–2 cm above the outlet pipe to prevent the substrate from being removed from the column. The synthetic wastewater with the physicochemical properties given in Table 2 was introduced to the CWs in down to up flow mode.

Three columns were constructed with a total working height of 30 cm and were labeled CWs-C1 to CWs-C3. The column of CWs-C1 contained media with four layers (up to down): 2 cm of sand (1.5–2.5 mm), 5 cm of fine gravel as the top layer (3–5 mm), 13 cm of alum sludge as the middle layer (5–7 mm), and 7 cm of coarse gravel as the bottom layer (8–12 mm); the column of

CWs-C2 had the same media patterns as those of CWs-C1 except for the insertion of two ACC electrode anodes and cathodes within the alum sludge layer and sand layer, respectively; and the CW-C3 column contained the same layer patterns as those of columns CWs-C2 except for two alum sludge layers in the column: 1 cm of sand, 4 cm of first alum sludge, 8 cm of coarse gravel, 7 cm later alum sludge, and 5 cm of coarse gravel with the insertion of the ACC cathode electrode and anode electrode, respectively, in the first and second alum layers. To deliver uniform synthetic wastewater into the columns, a fine bubble shower with a peristaltic pump was used. The applied potentials for columns of CWs-C2 and CWs-C3 were adjusted in the range of 0.2 to 1 V *vs.* Ag/AgCl. All the columns were planted with lentil plants (*Lens culinaris*). The plants were first seeded in sterile Petri dishes, and after they were grown and germinated, they were transplanted into columns. The fine sands of the CWs-C1 and CWs-C2 columns and first alum sludge layer in the column of CWs-C3 are aerated through fine diffusers with an aquarium pump to actively allow oxygen from the atmosphere in the mentioned layers and prevent further limitation of oxygen in those layers. A perforated hole was created on the opposite side of the influent aeration to prevent the diffusion of oxygen to other layers. Artificial sunlight was used to expose the reactors to simulated sunlight at an ambient temperature of nearly 25 °C. The system was operated continuously for 70 days. After this period, no significant removal of parameters was observed. Prior to this, a start-up period of two weeks was implemented to allow for acclimatization and the development of



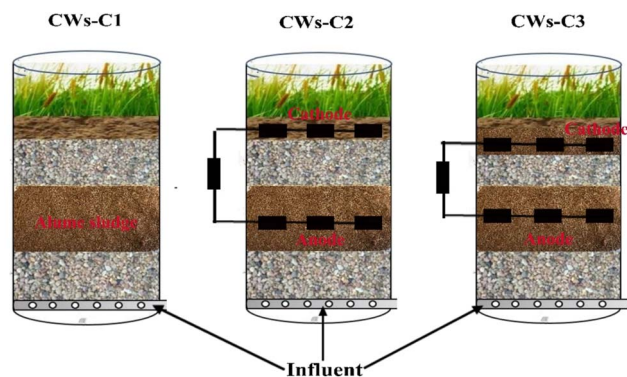


Fig. 1 Schematic diagram of the substrate and inserted electrodes in as-prepared CWs.

Table 2 The synthetic wastewater properties and studied parameters of column tests

Parameters	Units	Value
COD	mg L <sup>-1</sup>	500 ± 11.2
TP	mg L <sup>-1</sup>	5 ± 0.81
NH <sub>4</sub> <sup>+</sup>	mg L <sup>-1</sup>	20 ± 0.58
NO <sub>3</sub> <sup>-</sup>	mg L <sup>-1</sup>	30 ± 1.1
Loading rate	m <sup>3</sup> m <sup>-2</sup> d <sup>-1</sup>	0.2
HRT	d	2
pH	—	7.1 ± 0.21
Applied potential	V	0.2–1
C/N ratio	—	1 to 15
DO	mg L <sup>-1</sup>	2.22–3.14

microorganisms over the media within the systems. All reactors were operated at a loading rate of 0.2 m<sup>3</sup> m<sup>-2</sup> d<sup>-1</sup> with an HRT of 2 days.

In this study, by assuming the formation of biofilms on ACC and alum sludge and other possible layers *via* the application of an external current to stimulate and accelerate the growth of microorganisms and alum sludge, an inoculation and cultivation step was performed for two weeks. In this phase, all the columns were inoculated with a mixture of anaerobic and aerobic activated sludge from a wastewater treatment plant as the initial culture medium, which was placed in Tehran, Iran. The mixture of sludge was mixed with synthetic wastewater at a ratio of 1 : 10 (V/V) and pumped into the reactor. The synthetic wastewater prepared in this study contained the following components: glucose, 0.502 g L<sup>-1</sup>; NH<sub>4</sub>Cl, 0.520 g L<sup>-1</sup>; NaNO<sub>3</sub>, 0.090 g L<sup>-1</sup>; NaCl, 0.031 g L<sup>-1</sup>; K<sub>2</sub>HPO<sub>4</sub>, 0.033 g L<sup>-1</sup>; and 5 mL of wolf vitamin solution and 10 mL wolf mineral solutions (more details about the prepared recipe are given in the ESI (Table S1†)). The average values (mg L<sup>-1</sup>) of chemical oxygen demand (COD), total phosphorous (TP), ammonium nitrogen (NH<sub>4</sub><sup>+</sup>-N), and nitrate-nitrogen (NO<sub>3</sub>) were 500, 5, 20, and 30, respectively. The initial pH of the synthetic wastewater was adjusted to 7–7.3 by adding an appropriate 50 mM phosphate buffer solution (Table S2†). Before the formal operation experiment started, the CWs were inoculated for two weeks (cultivation) to provide a suitable adaptation microenvironment for microbial and

plant growth within the CWs, which was refreshed every 2 days. The operation experiments were run with the same composition and different C/N ratios, ranging from 2 to 15.

### 2.3. Sample collection and analysis

To evaluate the effects of inserting anode and cathode electrodes in CW systems, water samples from influent and effluent reactors were collected daily. The collected samples were passed through a 0.45 μm membrane and then preserved at 4 °C before analysis. The COD, NO<sub>3</sub><sup>-</sup>-N, NH<sub>4</sub><sup>+</sup>-N, and TP contents were analyzed *via* the colorimetric method with a UV/VIS spectrophotometer according to standard methods.<sup>18</sup> The pH, electrical conductivity, temperature, and dissolved oxygen (DO) content were measured *in situ*. All experimental measurements were performed in triplicate, and the results are expressed as average values.

The biofilm formed on the electrodes was observed by scanning electron microscopy (SEM) at the end of the experiment. The samples were cut into small portions and prepared before observation as follows: the electrodes were fixed in 2% glutaraldehyde (GA) or 2.5% paraformaldehyde solutions overnight at 4 °C. Dehydration of the samples was then performed with 40, 50, 60, 70, 80, 90, 100, or 100% (v/v) ethanol for 20 min. Finally, the dehydrated samples were dried in air overnight and then coated with a thin layer of palladium–gold to obtain SEM images.<sup>19</sup>

### 2.4. Characterization of biochar and alum sludge

A scanning electron microscope (SEM) coupled with EDAX (Hitachi, S-3500 N) was used to investigate the surface morphology and elemental distribution, respectively. The types of bonding and functional groups present in the biochar and alum sludge were determined *via* an IR spectrometer in the range of 4000–600 cm<sup>-1</sup>. The specific surface area and porosity were studied *via* BET analysis (Table S3†).

### 2.5. Microbial community analysis

The formed biofilms on the electrodes inserted into substrates in CWs-C2 and CWs-C3 reactors were rinsed using saline phosphate buffer (SPB) after collecting at the end of operation experiments and after centrifuging at 10 000 rpm for 10 min, were stored at –80 °C. The samples were submitted to Faculty of the Division of Cell and Molecular Biology, University of Tehran, Iran for DNA extraction and Illumina MiSeq high-throughput sequencing using Illumina platform PE250 model. The microbial community and their structures were analysed and clustered into the operational taxonomic units (OTUs) by performing the UPARSE software at 97% similarity (UPARSE OTU clustering (<https://www.drive5.com>)). Data with the confidence threshold of 0.7 was considered according to the Silva database. Lastly, the microbial composition of samples was estimated according to obtained information from OTUs at the taxonomic level.

### 2.6. Statistical analysis

SPSS 22.0 was used to analyze the obtained data, and Origin Pro 2021 was used to plot the data.



### 3. Results

#### 3.1. Effects of applied potential and evaluation of pollutant removal in CWs

By placing electrodes into the substrates of CWs and applying potential, CWs behave differently than those without electrodes and those with two alum sludge substrates. This behavior can be observed for organic compounds such as COD removal in CWs. When the CW-C1 reactor was operated without an electrode, the average removal of COD was 68%. COD removal was significantly enhanced by the coupling electrode and applied potential, as shown in Fig. 2a, for the CW-C2 and CW-C3 systems at different applied potentials, with significant differences. The CW-C2 reactor with electrodes inserted into a single layer of alum sludge reached average COD removal rates of 70%, 78%, and 69.3% when the applied potential was increased to 0.2 V, 0.6 V, and 1 V *vs.* Ag/AgCl, respectively. These results confirmed that the application of potential was able to induce the acclimation of the electrode surface biofilm.<sup>20</sup> Moreover, applying a potential can increase the electron affinity of the anode electrode,<sup>21</sup> which in turn leads to an electromotive force that drives more and significantly more electrons to flow into the anode and enhances the growth of microorganisms and the degradation of organic matter (Fig. S1†). However, the COD removal values decreased to 70% and 69.3%, respectively, when the CW-C2 reactor was operated at lower (0.2 V *vs.* Ag/AgCl) and higher (1 V *vs.* Ag/AgCl) potentials than the ideal 0.6 V *vs.* Ag/AgCl potential. It can be posited that anode potential values greater than 0.6 V *vs.* Ag/AgCl (here, study) generated a very thin

anode biofilm with low microbial density, which may be demolished due to lower stability, whereas anode potential values less than 0.6 V *vs.* Ag/AgCl (this study) can preferentially choose specific microorganisms, such as Geobacteraceae-like cells, and form a high density of cells and very thick biofilms.<sup>22</sup> An appropriate anode biofilm thickness and microbial density and diverse biofilms could be achieved by applying 0.6 V *vs.* Ag/AgCl anodic potential.

Compared with CWs-C2, CWs-C3 reactors with two layers of alum sludge and inserting ACC cathode and anode electrodes into the first and second alum layers (from perspective up to down), respectively, exhibit a higher COD removal rate when the applied potential is increased to 1 V *vs.* Ag/AgCl. As shown in Fig. 2a, CWs-C3 experienced a higher average COD removal of 87.11% at an applied potential of 1 V *vs.* Ag/AgCl than 80% and 74% at 0.6 and 0.2 V *vs.* Ag/AgCl, respectively. The insertion of two layers of alum sludge in CWs can significantly decrease organic matter degradation, which is consistent with other reported studies.<sup>23</sup> The inclusion of two alum sludge layers can act as an active and adsorptive layer to induce organic matter to be removed collectively from wastewater *via* various mechanisms, such as adsorption, chemical oxidation or reduction, hydrolysis, and microbial degradation.<sup>24</sup> By inserting a cathode electrode into alum sludge first and, with respect to the benefit of alum sludge, the coexistence of electroactive and aerobic bacteria over the cathode electrode and the formation of microbial biofilms with increased occupancy and variety can be posited as one of the reasons for the greater potential for achieving higher removal rates. The measured biomass results

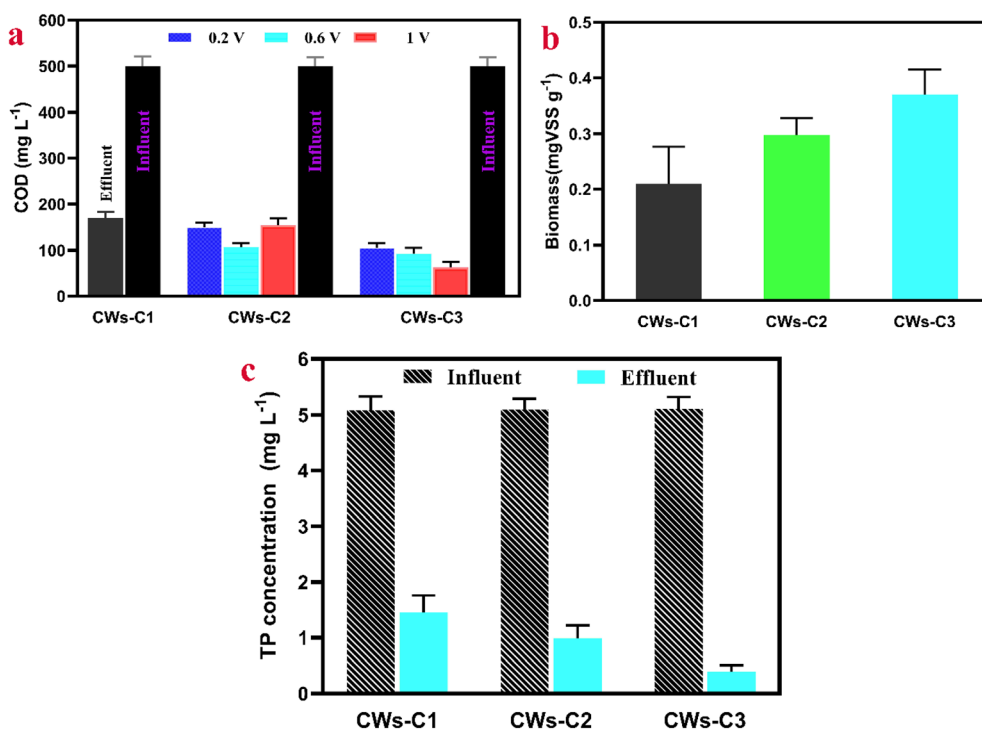


Fig. 2 (a) The averages of Removal performance of COD in different systems; (b) the biomass values for as-prepared reactors; and (c) the averages of removal performance of TP in reactors (note: the performance of TP in CWs-C2 and CWs-C3 were investigated at applied potential 1 V (*versus* Ag/AgCl)) (note: the operation period for all parameters were 45 days with HRT of 2 days, every 5 days parameters were measured).



(Fig. 2b) also verified the greater microbial density of the ACC cathode inserted in the first alum layer in the CW-C3 reactor than in that inserted in the sand layer in the CW-C2 reactor. Moreover, the important role of the cathode and anode ACC electrodes in the CWs-C3 reactor was notably the growth of biofilms, which was significantly greater in CWs-C3 than in CWs-C2, indicating a variety of bacterial cells, compositions of polymeric substances and cell growth over ACC electrodes.<sup>25</sup>

The trends in the TP and total nitrogen ( $\text{NH}_4^+$  and  $\text{NO}_3^-$ ) removal efficiencies were consistent with the trends in the COD removal efficiency. As is well known and verified in many studies,<sup>26</sup> P removal from wastewater in CWs is strongly influenced by the substrates used, as alum sludge has a high adsorption capacity for P removal. Additionally, as shown in Fig. 2c, in the CWs-C3 reactors, P removal was greater (77%) than that in the CWs-C2 reactors (65%) at higher applied potentials (here, 1 V *vs.* Ag/AgCl). Notably, the applied lower potential in this work (1 V *vs.* Ag/AgCl) is lower than that of water electrolysis (theoretically 1.23 V *vs.* Ag/AgCl), so  $\text{O}_2$  generation at the cathode of CWs is neglected. P removal at higher potentials can be considered to release more  $\text{Al}^{3+}$  or  $\text{Fe}^{3+}$  from alum sludge, which could form  $\text{FePO}_4$  or  $\text{AlPO}_4$  to remove P effectively.<sup>27</sup> Moreover, increasing the release of dissolved  $\text{Al}^{3+}$  or  $\text{Fe}^{3+}$  ions and further combining with  $\text{OH}^-$  in water or ACC surfaces (Fig. S2a†) and consequently forming  $\text{AlOOH}$  or  $\text{FeOOH}$  is another reason for the increased P removal efficiency.<sup>28</sup> This was further verified by obtaining FT-IR spectra of alum sludge from the CWs-C2 and CWs-C3 reactors (Fig. S2b†).

The  $\text{NH}_4^+$ -N removal rates of the CWs-C3 reactor were higher (83%) than those of the CWs-C1 (43.8%) and CWs-C2 (61%)

reactors at the optimum application potential of 0.6 V *vs.* Ag/AgCl.  $\text{NH}_4^+$ -N can be removed *via* adsorption to the abundant negatively charged functional groups of biochar and microbial assimilation by nitrifying bacteria.<sup>29</sup> Compared with other applied potentials, CWs-C3 enhanced the removal of  $\text{NH}_4^+$ -N at 0.6 V *vs.* Ag/AgCl because a higher applied potential could disturb the charge balance in biochar-doped electrodes and microbial attachments and positively charged  $\text{NH}_4^+$ -N.<sup>30</sup> Thus, a medium applied potential (here, 0.6 V *vs.* Ag/AgCl) suggested that both physical and/or chemical adsorption and microbial assimilation caused by rapid growth and reproduction of nitrifying bacteria can effectively contribute to higher removal rates of  $\text{NH}_4^+$ -N. The predominant physical or/and chemical adsorption of  $\text{NH}_4^+$ -N in the CW-C1 reactor results in lower removal rates of  $\text{NH}_4^+$ -N (43.8%). As the growth of nitrifiers over the ACC electrode in CWs-C2 is lower than that over CWs-C3, the potential applied over the ACC electrode could decrease the negative charge and cation exchange capacity of biochar,<sup>31</sup> as shown in Fig. 3a. It is believed that the insufficient supply of organic carbon in the shortest period of time of wastewater flow in the biochar ACC cathode inserted in the CWs-C2 reactor compared with that in the CWs-C3 reactor could limit the completion of nitrification, resulting in lower removal rates of  $\text{NH}_4^+$ -N in CWs-C2. The abundance of Proteobacteria, which included various groups of nitrifier microorganisms, was greater in CWs-C3 than in CWs-C2 (Fig. 6 and 7). The sufficient retention time and organic matter in the first layer of alum sludge used as the cathode ACC electrode of the CW-C3 reactor, which effectively accumulates and facilitates microbial growth

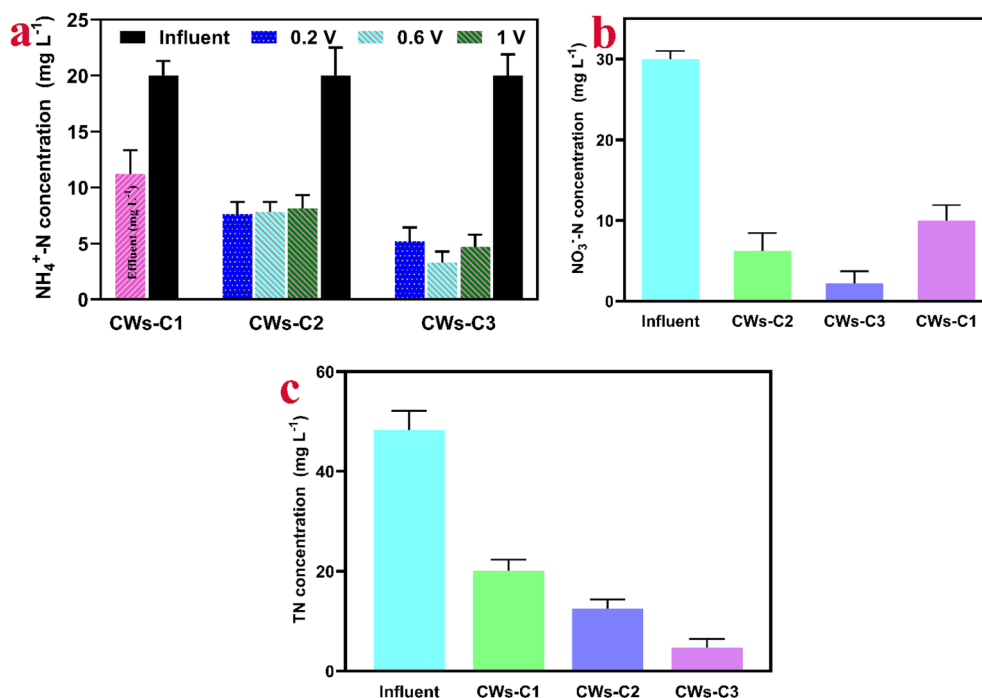


Fig. 3 (a) The performance of CWs in the  $\text{NH}_4^+$ -N removal at different applied potential; (b) and (c) the  $\text{NO}_3^-$ -N and TN removal at constant applied potential of 0.6 V (*versus* Ag/AgCl). (note: the operation period for all parameters were 45 days with HRT of 2 days, every 5 days parameters were measured).



and biofilm formation, can accelerate nitrification and significantly increase  $\text{NH}_4^+\text{-N}$  removal in the CW-C3 reactor.

The complete nitrification and further accumulation of appropriate  $\text{NO}_3\text{-N}$  in the anode section of the CW-C3 reactor as an electron acceptor caused higher removal rates of  $\text{NO}_3\text{-N}$  and total nitrogen (TN) in the CW-C3 reactor than in the CW-C1 and CW-C2 reactors (Fig. 3b and c).

### 3.2. Effects of the C/N ratio

The average removal rates of COD in CW reactors are significantly influenced by different C/N ratios, as shown in Fig. 4a. For the CWs-C1 reactor, the average removal rates of COD slightly increased with increasing C/N ratios from 2 to 6. Notably, the CW-C1 reactor benefited enormously from the application of the alum sludge layer as a substrate to CWs because of the adsorption of organic matter and further accumulation of more microbial density, resulting in higher COD removal rates. The COD removal rates significantly change at C/N ratios greater than 6, suggesting that the high accumulation of organic matter could lead to a high F/M ratio and further decrease the activity of microorganisms.<sup>32</sup>

Inserting the ACC electrode and applying potential into the CWs-C2 and CWs-C3 reactors could be considered reasons for both the higher average COD removal rates and the higher C/N ratios (Fig. 4a). The high porosity of biochar-doped ACC electrodes and the formation and growth of microorganisms massively and variously promoted the removal rates of COD at high C/N ratios. However, higher COD removal rates (96% vs. 85%) and higher C/N ratios (10 vs. 8) were observed in CWs-C3 than in CWs-C2, suggesting that the advantages of inserting an ACC cathode in the first layer of alum sludge in CWs-C3 reactors than in the sand layer of CWs-C2 could be related to the advantages of inserting an ACC cathode.

Notably, a balance should exist between the C/N ratio and the removal rate of  $\text{NH}_4^+\text{-N}$  and  $\text{NO}_3\text{-N}$ . As reported earlier,<sup>33</sup> at lower C/N ratios, a lack of enough organic matter sources as electron donors' results in incomplete growth and reproduction of nitrifying bacteria. However, the microbial community and diversity were the lowest, particularly the relative abundance of Proteobacteria, due to the fast growth and dominance of heterotrophic bacteria at relatively high C/N ratios. Fig. 4b

clearly shows that the best removal efficiency of TN ( $\text{NH}_4^+\text{-N}$  and  $\text{NO}_3\text{-N}$ ) in the CW-C1 system (58%) was achieved at a C/N ratio of 6. However, higher C/N ratios were observed for the CWs-C2 (74%) and CWs-C3 (89%) reactors (C/N ratios of 8/1 and 10/1, respectively), suggesting that the inclusion of biochar-doped ACC electrodes with potential and increased abundance of nitrifying and denitrifying bacteria in the cathode and anode parts of CWs, respectively, could be possible reasons for the increased C/N ratios in the influent flow of wastewater in this study compared with those in other studies.<sup>34</sup> Equally importantly, the  $\text{Fe}^{2+}$  released from alum sludge layers can act as an electron donor that can induce autotrophic denitrifying bacteria for nitrate reduction.

### 3.3. Microbial community in the operated reactors

Different configurations of alum sludge substrates and biochar-doped ACC electrodes with different application potentials were used in CW reactors, and their effects on the enhancement of organic matter and nutrient removal efficiency from synthetic wastewater were assessed. As mentioned earlier, the highest diversity and richness of the microbial community were observed in the CW-C2 and CW-C3 reactors at potentials of 0.6 and 1 V vs. Ag/AgCl, respectively, for the highest removal rates of COD; 0.6 V vs. Ag/AgCl for the  $\text{NH}_4^+\text{-N}$  and  $\text{NO}_3\text{-N}$  removal efficiencies for both reactors; and C/N ratios of 8 and 10 for both reactors (Table 3). According to the microbial community composition shown in Fig. 5, the relative abundance of Proteobacteria in the cathode parts of CWs-C3 (20.23–24.36%) was greater than that in the CWs-C2 reactor (16.89–19.87%), suggesting that the use of alum sludge substrate as the cathode parts and the simultaneous application of potential could

Table 3 The diversity and richness of sample flora in CWs reactors

Reactors	ACE	Chao 1	Shannon	Simpson	Coverage
CWs-C1 (cathode)	1559.18	1571.27	1.76	0.051	0.99
CWs-C1 (anode)	1589.96	1593.49	1.82	0.026	0.99
CWs-C2 (cathode)	1885.01	1888.17	1.97	0.028	0.99
CWs-C2 (anode)	1662.70	1695.86	1.74	0.023	0.99
CWs-C3 (cathode)	2137.98	2144.18	2.11	0.028	0.99
CWs-C3 (anode)	1872.67	1880.25	1.82	0.044	0.99

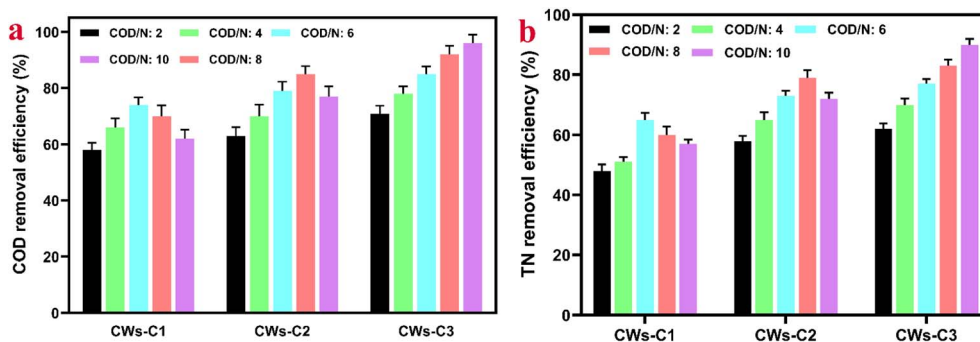


Fig. 4 The removal efficiency of (a) organic matters; and (b) TN at different COD/N ratios (note: the operation period for all parameters were 45 days with HRT of 2 days, every 5 days parameters were measured).



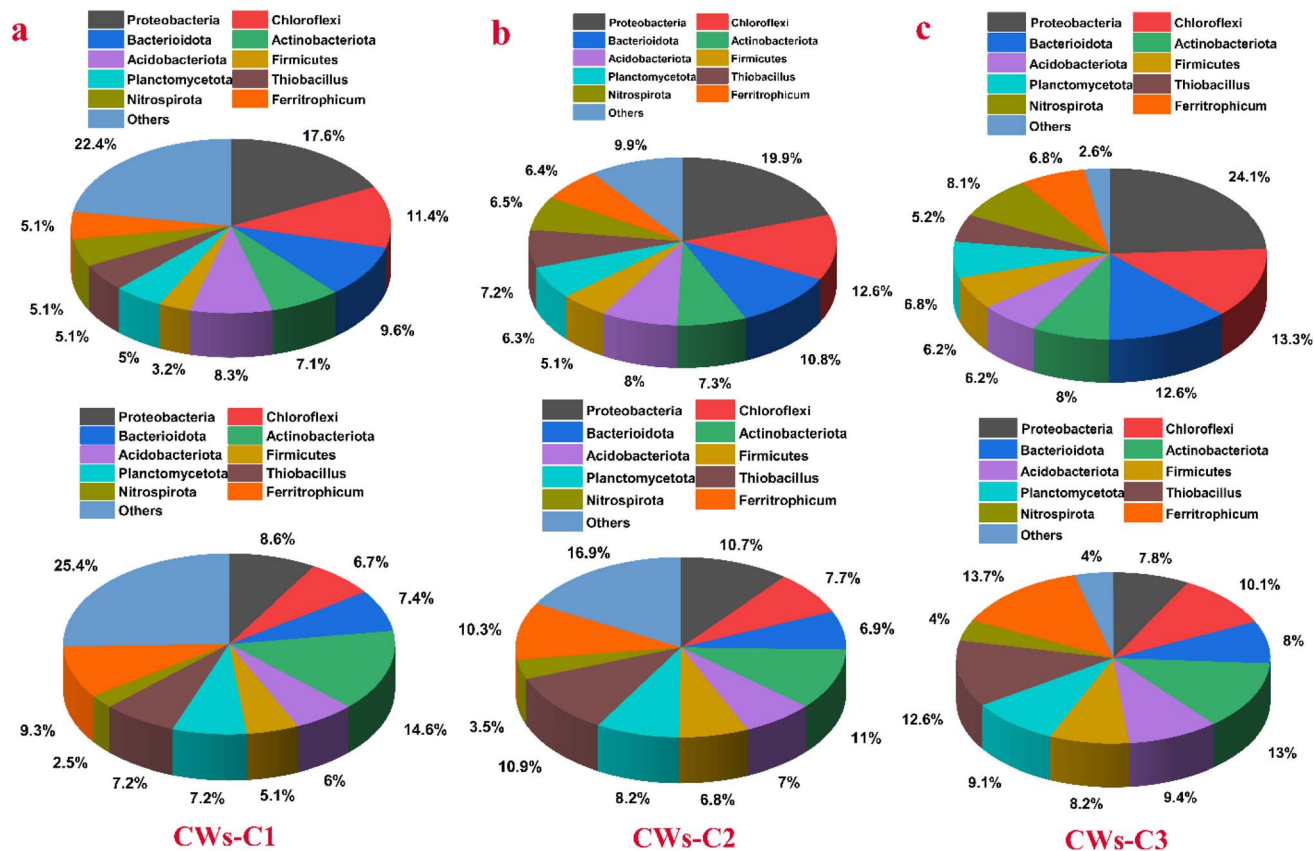


Fig. 5 Microbial community analysis of reactors at the phylum levels (Note: in all reactors, the top plots represent the cathode parts and bottom plots represent the Anode parts of CWs reactors.).

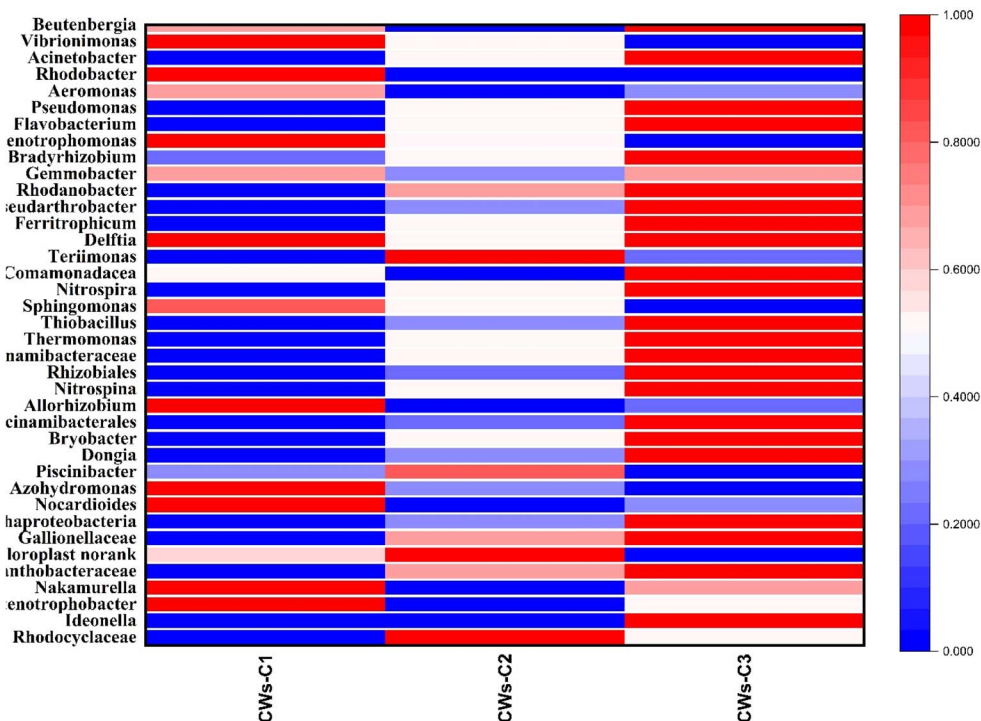


Fig. 6 The microbial communities at the genus level at different reactors.



increase the variety of microorganisms with nitrification ability belonging to this group. Among the other groups, Bacteroidetes, which included nitrite bacteria, nitrate bacteria, and denitrifying bacteria, represented the highest proportion in the CWs-C3 reactor. Moreover, the presence of Chloroflexi at higher abundances in CWs-C3 than in CWs-C2 significantly increased the removal rates of COD and TN in the CWs-C3 reactor because of their ability to utilize organic matter for photosynthesis and  $\text{NH}_4^+$ -N and organic N for growth as nitrogen sources.<sup>35</sup>

The dominant genera of the microbial community are also illustrated in Fig. 6, which shows that the genera belonging to N and Fe included alum sludge, and electrochemically active bacteria (EAB) were significantly different between the CW-C2 and CW-C3 systems. The dominant genera were Saccharimonadales, norank, Acinetobacter, Pseudomonas, Rhodobacter, and Desulfobacterota. The relative abundance of genera related to nitrification and denitrification was predominant in the CW-C3 reactor, indicating that the use of two alum sludge layers as substrates and the application of electrical potential strongly promoted the removal of N and organic matter by changing the structure of N transformation and the organic matter of degrading bacteria. The main nitrifier bacteria (Nitrospira and Nitrospina) were found to be more abundant in the cathode ACC electrode of CWs-C3 than in the cathode region of CWs-C2 (Fig. 7). The alum sludge substrate and its advantages mentioned earlier and the use of  $\text{Fe}^{2+}$ -containing alum as an electron donor may increase the metabolism and activity of microorganisms.<sup>36</sup> Owing to relatively appropriate nitrification in the cathode of CWs-C3, more denitrifying bacteria were present in the anode region of CWs-C3 than in the CW-C2 reactor. Therefore, the greater opportunity to reduce  $\text{NO}_3^-$ -N in the anode region of the CWs-C3 reactor could effectively increase the TN removal rate compared with the TN removal rates in the CWs-C2 reactor.

In addition, the microbial community related to Fe(II) autotrophic denitrifying bacteria, such as Ferritrophicum and Thiobacillus, was more abundant and diverse in the anode region

of the CW-C3 reactor, which significantly reduced  $\text{NO}_3^-$ -N, and further TN removal was effectively enhanced in the CW-C3 reactor. The increased abundance of Pseudomonas in the anode region of the CWs-C3 reactor indicates appropriate P removal rates in which applying potential had a moderate effect on P-accumulating bacteria. The presence of EABs in the anode region highlights the important role of interspecies species in enhancing organic matter and nutrient removal in CWs-C2 and CWs-C3 reactors.

#### 3.4. N and P removal mechanisms in CWs-C3

When a potential of 1 V vs. Ag/AgCl was applied to alum sludge containing a biochar-doped ACC electrode, the Fe and Al ions released from alum sludge formed  $\text{FePO}_4$  and  $\text{AlPO}_4$  *in situ* because of interactions with phosphate in wastewater, which promoted high percentages of P removal in the CW-C3 reactor. The greater intensity of bond adsorption at  $1030\text{ cm}^{-1}$  in CWs-C3 corresponds to Fe–O–P vibrations (Fig. S2†). The intensity of the O–H stretching vibration at  $3465\text{ cm}^{-1}$  and O–H bending vibration at  $1620\text{ cm}^{-1}$  and the absorption band near  $820\text{ cm}^{-1}$  correspond to Fe–OH or Al–OH bonds, indicating that the released Al and Fe ions could combine with  $\text{OH}^-$  near the biochar-doped ACC electrode, generate  $\text{AlOOH}$  or  $\text{FeOOH}$  and consequently interact with phosphorous in wastewater.

In addition, the high contribution of Fe autotrophic denitrifying bacteria in the CWs-C3 reactor, such as Ferritrophicum and Thiobacillus, suggested that  $\text{Fe}^{2+}$  as an electron donor and  $\text{Fe}^{3+}$  as an electron acceptor due to significant redox cycles can play important roles in the denitrification process. A proposed schematic of the simultaneous mechanism of TN and TP removal in CWs-C3 by focusing on the application of alum sludge as a substrate and inserting an ACC electrode as an inducer and stimulator of initial mechanisms and microbial growth is shown in Fig. 8.

In conclusion, the placing alum sludge substrate in CWs-C3 plays a crucial role in the initial breakdown, transformation of organic matters, effective nitrification and subsequently denitrification. So, the degradation of organic matter and the

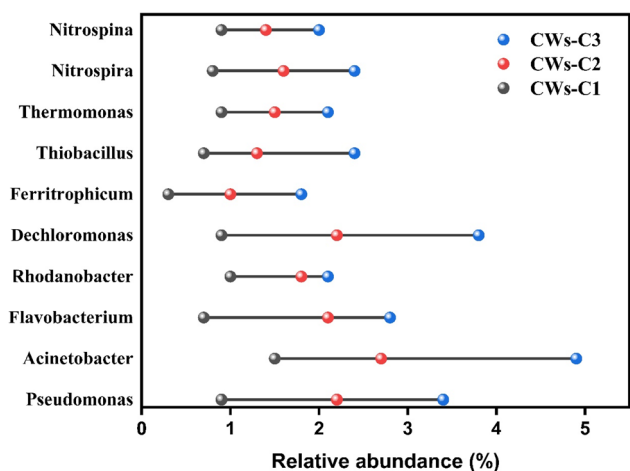


Fig. 7 The microbial genera involved in TN conversion at different reactors.

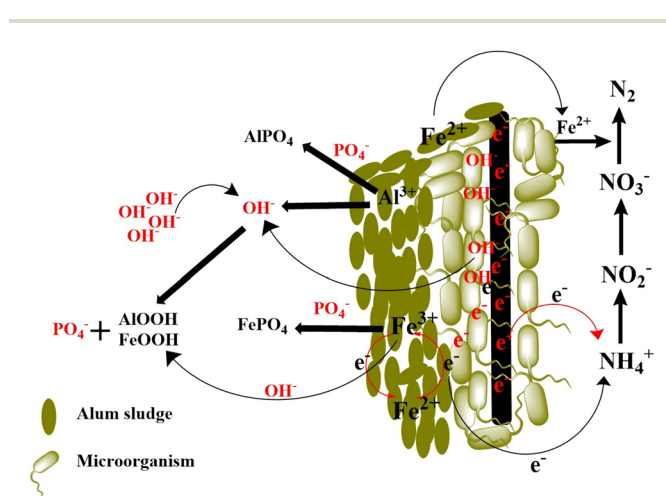


Fig. 8 The proposed mechanism of synergistic removal of TN and TP.



conversion of ammonium to nitrate and nitrogen gas can be enhanced, significantly contributing the reduction of COD and TN. The redox reactions and enhanced microbial activity induced by placing electrodes within the CWs-C3 can lead to the degradation of organic matters, transformation of nitrogen compounds, and the adsorption and precipitation of phosphorus compounds. Moreover, the alum sludge as substrate provides ideal adaption place for microorganisms and also a robust adsorptive capacity for phosphorus, leading to significant TP removal. The adsorption process captures residual pollutants that may not be fully degraded by biological or electrochemical mechanisms, thereby enhancing the overall removal efficiency of COD, TN, and TP. To sum up, the alum sludge-driven electro-phytoremediation approach integrates biological action, electrochemical effects, and adsorption to provide a comprehensive and efficient solution for nutrient removal. Each mechanism contributes uniquely to the removal of COD, TN, and TP, resulting in a sustainable and high-performance CWs systems. Further optimization and research are essential to maximize the potential of these integrated processes and address the complexities of wastewater treatment.

## 4. Conclusion

Simultaneously, significant mitigation of organic matter and nutrient-rich wastewater was carried out in CWs designed with alum sludge substrate, and potential was applied to biochar-doped ACC electrodes. The results demonstrated that alum sludge as a substrate and the application of potential could change the microbial diversity and density toward completing nitrification and denitrification and highly biodegraded organic matter. Owing to the iron- and aluminum-containing alum sludge, TP can be mitigated predominantly by the formation of Fe/AlPO<sub>4</sub> or Al/FeOOH-P interactions. Moreover, the released Fe ions can act as electron donors and serve as Fe-driven autotrophic denitrifiers, consequently increasing the TN removal efficiency. To conclude, appropriately designing and utilizing waste material as a substrate in CWs and applying a driving stimulator to promote microbial growth and microbial diversity can be promising strategies for simultaneously promoting organic matter and nutrients and utilizing CWs on a large scale and in practical applications. The findings obtained in our study can be conducive to the application of CWs for wastewater treatment, with all the benefits mentioned above.

## Data availability

Data for this article are available at Origin 2024b [<https://www.originlab.com/2024b>]. Data supporting this article have been included as part of the ESI.†

## Conflicts of interest

There are no conflicts to declare.

## Acknowledgements

The authors gratefully acknowledge the financial and technical support provided by the Baqiyatallah University of Medical Sciences. This research was approved by the Ethics Committee of Baqiyatallah University of Medical Sciences (IR.BM-SU.REC.1402.064) and project number # 401000559.

## References

- (a) H. Guven, M. Ersahin, H. Ozgun, I. Ozturk and I. Koyuncu, *J. Environ. Manage.*, 2023, **329**, 117130; (b) M. Faisal, K. M. Muttaqi, D. Sutanto, A. Q. Al-Shetwi, P. J. Ker and M. Hannan, *Renew. Sustain. Energy Rev.*, 2023, **181**, 113324; (c) J. Arámbula, S. Mohammadi, A. Mahdaviarab, D. Sanaei, R. P. Patil and H. Sharifan, *New J. Chem.*, 2023, **47**, 22235–22245.
- M. H. Dehghani, D. Sanaei, I. Ali and A. Bhatnagar, *J. Mol. Liq.*, 2016, **215**, 671–679.
- (a) M. Sarmadi, M. Foroughi, H. Najafi Saleh, D. Sanaei, A. A. Zarei, M. Gahrchi and E. Bazrafshan, *Environ. Sci. Pollut. Res.*, 2020, **27**, 34823–34839; (b) W. Piao, Y. Kim, H. Kim, M. Kim and C. Kim, *J. Clean. Prod.*, 2016, **113**, 325–337; (c) S. M. Rahman, M. J. Eckelman, A. Onnis-Hayden and A. Z. Gu, *Environ. Sci. Technol.*, 2016, **50**, 3020–3030; (d) R. Boiocchi and G. Bertanza, *Water Sci. Technol.*, 2022, **85**, 1673–1687.
- (a) G. Rodriguez-Garcia, N. Frison, J. Vázquez-Padín, A. Hospido, J. Garrido, F. Fatone, D. Bolzonella, M. Moreira and G. Feijoo, *Sci. Total Environ.*, 2014, **490**, 871–879; (b) T. Sampedro, L. Gómez-Coma, I. Ortiz and R. Ibañez, *Sci. Total Environ.*, 2024, **906**, 167154.
- (a) M. Yang, M. Peng, D. Wu, H. Feng, Y. Wang, Y. Lv, F. Sun, S. Sharma, Y. Che and K. Yang, *Resour. Conserv. Recycl.*, 2023, **190**, 106794; (b) Z. Liu, Z. Xu, X. Zhu, L. Yin, Z. Yin, X. Li and W. Zheng, *Sci. Total Environ.*, 2023, 169356; (c) V. Alevizos, I. Georgousis and A. Kapodistria, *Pollutants*, 2023, **3**, 521–543.
- (a) F. García-Ávila, A. Avilés-Añazco, R. Cabello-Torres, A. Guanuchi-Quito, M. Cadme-Galabay, H. Gutiérrez-Ortega, R. Alvarez-Ochoa and C. Zhindón-Arévalo, *Case Studies in Chemical and Environmental Engineering* 2023, vol. 7, p. 100307; (b) Z. Tao, Z. Jing, M. Tao, Y. Kong, L. Guan and Q. Jia, *Bioresour. Technol.*, 2023, **380**, 129075.
- M. M. Waly, T. Ahmed, Z. Abunada, S. B. Mickovski and C. Thomson, *Land*, 2022, **11**, 1388.
- F. Younas, N. K. Niazi, I. Bibi, M. Afzal, K. Hussain, M. Shahid, Z. Aslam, S. Bashir, M. M. Hussain and J. Bundschuh, *J. Hazard. Mater.*, 2022, **422**, 126926.
- (a) J. K. Tang, M. N. H. Jusoh and H. Jusoh, *Trop. Aquat. Soil Pollut.*, 2023, **3**, 76–87; (b) H. Wu, R. Wang, P. Yan, S. Wu, Z. Chen, Y. Zhao, C. Cheng, Z. Hu, L. Zhuang and Z. Guo, *Nat. Rev. Earth Environ.*, 2023, **4**, 218–234.
- (a) V. Carrillo, G. Gómez and G. Vidal, *Ecol. Eng.*, 2022, **182**, 106690; (b) L. Gong, X. Zhao and G. Zhu, *Sustainability*, 2022, **14**, 8819; (c) K. Kill, L. Grinberga, J. Koskiaho, Ü. Mander, O. Wahlroos, D. Lauva, J. Pärn and K. Kasak, *Ecol. Eng.*,



- 2022, **180**, 106664; (d) Y. Liu, L. Feng, Y. Liu and L. Zhang, *Environ. Sci. Pollut. Res.*, 2023, **30**, 23035–23046; (e) J. Li, B. Zheng, X. Chen, Z. Li, Q. Xia, H. Wang, Y. Yang, Y. Zhou and H. Yang, *Water*, 2021, **13**, 476.
- 11 V. Patyal, D. Jaspal and K. Khare, *Bioresour. Technol. Rep.*, 2024, **26**, 101870.
- 12 (a) A. Biswas and S. Chakraborty, *Sci. Total Environ.*, 2024, **912**, 168809; (b) D. Kumari and K. Dutta, *J. Environ. Chem. Eng.*, 2024, **12**, 113119; (c) Y. Kong, M. Tao, X. Lu, C. Cheng and Z. Jing, *Desalination Water Treat.*, 2024, **318**, 100358.
- 13 M. Tao, Y. Kong, S. Cao, Z. Jing, L. Guan, Q. Jia and Y.-Y. Li, *Chem. Eng. J.*, 2024, **487**, 150753.
- 14 D. Sanaei, M. Sarmadi, M. H. Dehghani, H. Sharifan, P. G. Ribeiro, L. R. Guilherme and S. Rahimi, *Environ. Sci.: Processes Impacts*, 2023, **25**, 2110–2124.
- 15 C. H. Ward, K. Balshaw-Biddle and C. L. Oubre, *Modular Remediation Testing Systems*, CRC Press, 1999.
- 16 EPA US, *Method 3050B: acid digestion of sediments, sludges, and soils*, Environ. Prot. Agency, 1996, vol. 2, pp. 3–5.
- 17 Y. Yang, Y. Zhao, A. Babatunde, L. Wang, Y. Ren and Y. Han, *Sep. Purif. Technol.*, 2006, **51**, 193–200.
- 18 (a) T. Hülsen, E. M. Sander, P. D. Jensen and D. J. Batstone, *Water Res.*, 2020, **181**, 115909; (b) A. P. H. Association, *Standard Methods for the Examination of Water and Wastewater*, American Public Health Association, 1926; (c) D. Sanaei, M. Massoudinejad, M. S. Javed, S. M. Zarandi, A. Rezaee, H. Sharifan and M. Imran, *J. Mater. Chem. C*, 2022, **10**, 1421–1435; (d) A. H. Mahvi, M. Sarmadi, D. Sanaei and H. Abdolmaleki, *Desalin. Water Treat.*, 2020, **200**, 205–216.
- 19 (a) N. Vyas, R. Sammons, O. Addison, H. Dehghani and A. Walmsley, *Sci. Rep.*, 2016, **6**, 32694; (b) A. Saavedra, D. C. Martínez-Casillas, J. R. Collet-Lacoste and E. Cortón, *J. Appl. Microbiol.*, 2023, **134**, lxad140.
- 20 J. A. Modestra, C. N. Reddy, K. V. Krishna, B. Min and S. V. Mohan, *Renew. Energy*, 2020, **149**, 424–434.
- 21 (a) A. Mirshafiee and A. Rezaee, *J. Water Proc. Eng.*, 2021, **44**, 102420; (b) S. Erazo and L. M. Agudelo-Escobar, *Processes*, 2023, **11**, 373.
- 22 C. I. Torres, R. Krajmalnik-Brown, P. Parameswaran, A. K. Marcus, G. Wanger, Y. A. Gorby and B. E. Rittmann, *Environ. Sci. Technol.*, 2009, **43**, 9519–9524.
- 23 (a) A. Omoike, *Water Res.*, 1999, **33**, 3617–3627; (b) W. Zhao, H. Xie, J. Li, L. Zhang and Y. Zhao, *Processes*, 2021, **9**, 612; (c) M. B. G. de Almeida, A. M. D. de Jesus, A. S. Pereira and F. A. Fiore, *J. Clean. Prod.*, 2024, **468**, 142975.
- 24 H. A. Nabwey and M. A. Tony, *Processes*, 2023, **11**, 2836.
- 25 S. Kumar, A. T. Nguyen, S. Goswami, J. Ferracane and D. Koley, *Sensor. Actuator. B Chem.*, 2023, **376**, 133034.
- 26 (a) D. Georgantas and H. Grigoropoulou, *Water Sci. Technol.*, 2005, **52**, 525–532; (b) N. Maqbool, Z. Khan and A. Asghar, *Desalination Water Treat.*, 2016, **57**, 13246–13254; (c) A. Babatunde, Y. Zhao and X. Zhao, *Bioresour. Technol.*, 2010, **101**, 6576–6579; (d) M. Pająk, *Int. J. Environ. Sci. Technol.*, 2023, **20**, 10953–10972; (e) A. Chen, L. Lv, R. Hu, X. Wei, J. Guan and X. Meng, *Sci. Total Environ.*, 2023, **867**, 161530; (f) Q. Ping, Z. Zhang, W. Guo, L. Wang and Y. Li, *Sci. Total Environ.*, 2024, **913**, 169641.
- 27 (a) Y. Lei, Z. Zhan, M. Saakes, R. D. van der Weijden and C. J. Buisman, *Water Res.*, 2021, **199**, 117199; (b) X. Ge, X. Cao, X. Song, Y. Wang, Z. Si, Y. Zhao, W. Wang and A. A. Tesfahunegn, *Bioresour. Technol.*, 2020, **296**, 122350; (c) A. Mielcarek, K. Ł. Bryszewski, J. Rodziewicz, K. Kłobukowska and W. Janczukowicz, *Energies*, 2024, **17**, 1352.
- 28 A. Shalaby, E. Nassef, A. Mubark and M. Hussein, *Am. J. Environ. Sci.*, 2014, **1**, 90–98.
- 29 (a) T. Abedi and A. Mojiri, *Environ. Technol. Innovat.*, 2019, **16**, 100472; (b) L. Feng, Z. Gao, T. Hu, S. He, Y. Liu, J. Jiang, Q. Zhao and L. Wei, *Chem. Eng. J.*, 2023, 144772; (c) L. Cheng, X. Gong, B. Wang, Z. Liu, H. Liang and D. Gao, *ACS ES&T Water*, 2024, **4**, 1834–1843; (d) H. Wang, Q. Chen, R. Liu, H. Xia and Y. Zhang, *J. Water Proc. Eng.*, 2023, **55**, 104170.
- 30 S. Farhangi-Abriz and K. Ghassemi-Golezani, *Chemosphere*, 2023, **313**, 137365.
- 31 D. V. Cuong, P.-C. Wu, N.-L. Liu and C.-H. Hou, *Sep. Purif. Technol.*, 2020, **242**, 116813.
- 32 M. Zhou, J. Cao, Y. Lu, L. Zhu, C. Li, Y. Wang, L. Hao, J. Luo and H. Ren, *Sci. Total Environ.*, 2022, **847**, 157569.
- 33 (a) W. Lu, Y. Zhang, Q. Wang, Y. Wei, Y. Bu and B. Ma, *Bioresour. Technol.*, 2021, **340**, 125661; (b) K. Hu, W. Li, Y. Wang, B. Wang, H. Mu, S. Ren, K. Zeng, H. Zhu, J. Liang and J. Xiao, *J. Water Proc. Eng.*, 2023, **53**, 103673; (c) D. Li, W. Li, D. Zhang, K. Zhang, L. Lv and G. Zhang, *Bioresour. Technol.*, 2023, **367**, 128254.
- 34 (a) D. Yao, N. Dai, X. Hu, C. Cheng, H. Xie, Z. Hu, S. Liang and J. Zhang, *Water Res.*, 2023, **243**, 120277; (b) X. Bai, J. Li and S. Chang, *Water*, 2023, **15**, 4272; (c) C. Xiang, Y. Du, W. Han, B. Guan, H. Liu, Y. An, Y. Liu, H. Jiang, J. Chang and Y. Ge, *Environ. Sci. Pollut. Res.*, 2024, **31**, 12036–12051.
- 35 P. Zhang, Y. Peng, J. Lu, J. Li, H. Chen and L. Xiao, *Chemosphere*, 2018, **211**, 25–33.
- 36 (a) H. Chen, X. Zhao, Y. Cheng, M. Jiang, X. Li and G. Xue, *Environ. Sci. Technol.*, 2018, **52**, 1404–1412; (b) B. Zhu, R. Yuan, S. Wang, H. Chen, B. Zhou, Z. Cui and C. Zhang, *J. Water Proc. Eng.*, 2024, **59**, 104952.

